Evidence from the Absorption and Emission Spectra of Trimethylenemethane Derivatives for Two Molecular Species in Thermal Equilibrium

Nicholas J. Turro,*[1a] Manfred J. Mirbach,[1a] Niels Harrit,[1a] Jerome A. Berson,*[1b] and Matthew S. Platz[1b]

Contribution from the Chemistry Department, Columbia University, New York, New York 10027, and the Chemistry Department, Yale University, New Haven, Connecticut 06520. *Received February 27, 1978*

Abstract: Photolysis of the bicyclic azoalkanes **2a** and **2b** in glassy organic solvents at temperatures near 77 K causes the appearance of new optical absorption spectra assigned to the trimethylenemethane derivatives **1a** and **1b,** respectively. The structural assignments are made on the basis of emission spectra, excitation spectra, theoretical calculation, and correlation of absorption and ESR data. In both instances, the optical spectra are best explained as properties of two species in thermal equilibrium.

Introduction

Many theoretical investigations have been undertaken recently to locate the electronic levels of trimethylenemethane (TMM) and its derivatives.[2,3] TMM maintains a unique position as a classic molecule treated in numerous texts on molecular orbital theory.[4] The intermediacy of TMM and its derivatives in many reactions is verified by the quite extensive studies on its thermal chemistry.[5] In spite of this, ESR spectroscopy[6] has served as the only means of direct physical detection of TMM and its derivatives. We wish to report the UV/vis absorption and emission spectra of the TMM derivatives **1a** and **1b.**

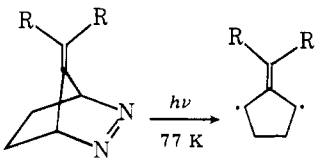

(1)

2a, R = Ph
b, R = CH_3
c, R = H

1a
1b
1c

Experimental Section

Absorption spectra were recorded on a Cary 17 spectrophotometer. Cryogenic temperatures were achieved by placing a quartz cell in an all-quartz Dewar which was continuously flushed with gaseous N_2. The latter gas was precooled by passage through a copper coil immersed in an external Dewar filled with liquid N_2. The optical path length of the cell was 1 mm. Temperature control was achieved by varying the rate of the N_2 flow. Temperature was monitored with a thermocouple placed in direct contact with the cell. **2a** was photolyzed by means of unfiltered light from a low-pressure mercury arc. In the case of **2b,** a 200-W Hg–Xe high-pressure source equipped with a Corning 7-37 filter (transmitting from 320 to 390 nm) was used. Emission and excitation spectra at 77 K were recorded on a Hitachi Perkin-Elmer MPF-3L spectrofluorimeter. In this case, samples were immersed directly into liquid N_2 in all-quartz Dewar. The corrected spectra published were achieved on a Schoeffel RRS 1000 spectrofluorimeter interfaced to a Tektronix 31A programmable calculator. Rhodamine B served as a quantum counter. In the case of **1b,** internal filter effects and interfering emission from starting material, photoproducts, or minor impurities were eliminated by subtracting consecutive spectra recorded before and after photolysis of **2b.** A single photon counting apparatus was used to determine the emission lifetime of **1a.** ESR spectra were recorded on a Varian E-4 spectrometer operated at 9 GHz (modulation frequency 1 kHz).

The glassy matrices employed in this study were 3-methylpentane (MP), methylcyclohexane (MCH), and the mixed solvents ether/isopentane/ethanol (EPA, volume ratio 5/5/2) and 1-propanol/2-propanol (1-P–2-P, volume ratio 2/3). All solvents were spectrograde (Matheson, Coleman and Bell) and were used without further purification. **2a** and **2b** were synthesized according to published procedures.[6c,d] **2b** was sublimed immediately before use.

Electronic Absorption and ESR Spectroscopy. Photolysis (254 nm) of **2a** in glassy matrices (MP, EPA, MCH, 1-P–2-P) at temperatures close to 77 K results in generation of a new species **1a,** as evidenced by the appearance of new absorption bands in the UV/vis region (Figure 1). The starting material **2a** absorbs at 300 and 343 (vibrational bands of the (n,π*) transition)[7] (ϵ^{343} 57 M^{-1} cm^{-1}) and at 251 nm (ϵ 1.0×10^4 M^{-1} cm^{-1}). The latter transition is assigned to the styrene chromophore and is the only band shown in Figure 1; i.e., the n,π* band is too weak to be seen under the conditions employed to display Figure 1. Excitation at 254 nm is seen to cause a gradual change from the spectrum of **2a** into a spectrum with intense bands in the 300–330-nm region as the most dominant feature. There is an isosbestic point at 270 (MCH) or 275 nm (EPA). This agrees with the relatively high photochemical and thermal stability of **1a,** (see below) since depletion of **1a** by secondary photolysis or by a thermal reaction that was slow in comparison to the time between scans would have precluded an isosbestic point.

Prolonged irradiation and increased sensitivity of the spectrophotometer permitted unambiguous detection of two weak bands between 450 and 500 nm. The relative intensities of these two bands are reversed, and there is a slight wavelength displacement, when EPA is used as glass. The spectral parameters are compiled in Table I. Estimated extinction coefficients are based on the depletion of the 251-nm absorption assuming that only one absorbing species is formed in 100% yield. This makes the value determined for the 330-nm peak a lower limit only. By manual extrapolation and integration of the main absorption band from ca. 250 to 350 nm an approximate oscillator strength f = 0.26 has been determined. The progression of the vibrational fine structure falls in the range 1050–1500 cm^{-1} but is random. Apparently either there is more than one vibrational mode involved or the band is composed of two electronic transitions.

The weak absorptions in the visible are evidently superimposed on the continuum stretching out from the ultraviolet. The extinction coefficients listed are *not* corrected for this and should be taken as only approximate if comparisons with theoretical calculations[3] are being made. An order of magnitude determination based on the assumption that absorption is due to a single species (vide infra, however) gives $f = 10^{-3}$–10^{-4} for the long-wavelength band of **2a** at 481 nm (EPA) (Figure 1). The isosbestic point from photolysis of **2a** observed was maintained until 50–75% conversion (Figure 1). In the final stages of photolysis the peak at 330 nm began to decrease without concomitant production of new absorption in the range open for observation. There was no indication of generation of the weak absorptions in the visible by "optical pumping" of the intense bands in the ultraviolet. On the contrary, synchronous behavior was observed for the buildup and for the disappearance (by secondary photolysis and also by thermal degradation) of both bands. The new absorption bands disappeared along with the softening of the glass upon heating and did not return upon cooling back to 77 K. Thus, **1a** is a transient that reacts

0002-7863/78/1500-7653$01.00/0

Table I. Spectroscopic Parameters for Substituted Trimethylenemethanes **1a** and **1b**

		Absorption							Emission		
	3-MP	260	287[a]	298	318	330	*b*	*b*			
	EPA	259	288[a]	296	314	328	451	481	484	510	EPA
1a	MCH	260	288[a]	299	315	329	440	480	488	512	MCH
						$\epsilon \geq 1.5 \times 10^4$ [c]					
	2-PrOH/1-PrOH (3:2)	258	288[a]	297	312	327	*b*	*b*			
	EPA		285[a]	299	308	322	405	428			
1b				$\epsilon \sim 250$			$\epsilon \sim 20$	$\epsilon \sim 13$			
	MCH				*b*		*b*		536	576	

[a] Shoulder. [b] Not investigated. [c] Extinction coefficients in units of M^{-1} cm^{-1}.

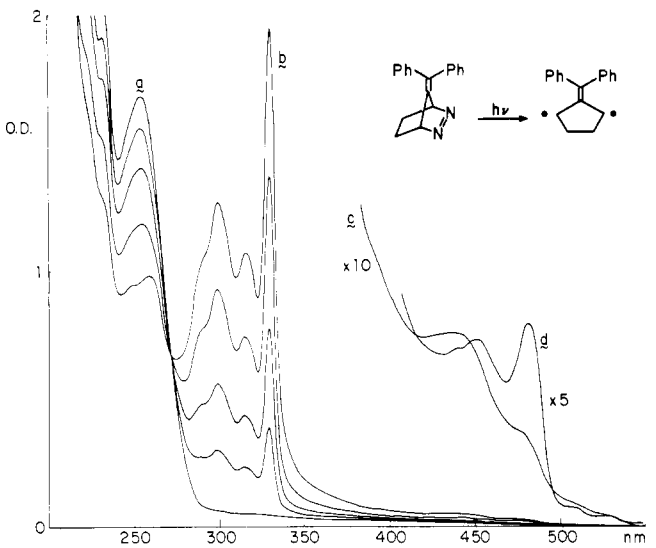

Figure 1. UV/vis spectra recorded during stepwise photolysis of **2a** at 79 K (a) before photolysis (Initial concentration in MCH at 300 K: 1.1×10^{-3} M). (b) same after a total of 290 s exposure (λ 254 nm) (Intermediate spectra shown). (c) same after 560 s exposure (expanded 10×). (d) spectrum (expanded 5×) after 86 min photolysis of a 1.1×10^{-2} M solution of **2a** in EPA.

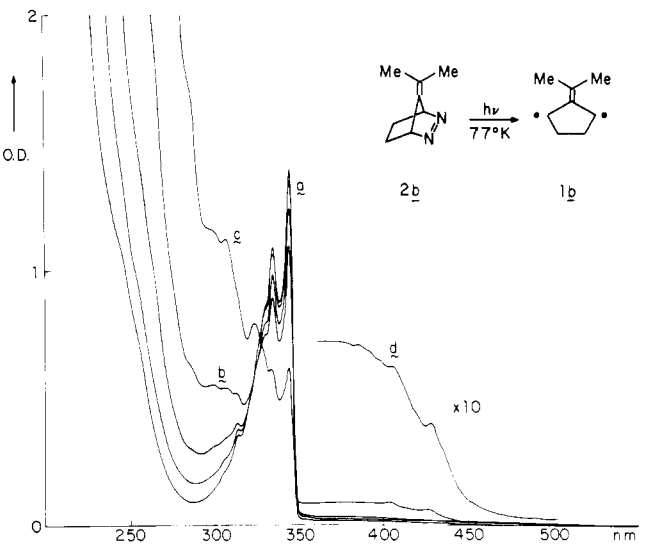

Figure 2. UV/vis spectra recorded during stepwise photolysis of **2b** in EPA at 79 K, concn (300 K) 7.8×10^{-2} M (a) before irradiation. (b) same after 10 min exposure (320 nm < λ < 380 nm). (c) same after 33 min exposure. (d) same after 47 min exposure (expanded 10×).

irreversibly when the glass melts. The temperature for onset and termination of the decay of **1a** varied with the nature of the glass, the thermal history of the sample, the rate of heating, and the initial concentration of the transient. Thus, in EPA, decay would typically start around 96 K and be terminated at 103–120 K. Macroscopic melting of EPA occurs at 140–150 K. Analogous behavior was observed for the other glasses. The spectrum of the thermal products derived from **1a** by melting the glassy matrix featured a continuum rising from 500 to 230 nm, upon which were superimposed two weak, broad maxima at ca. 340 and ca. 310 nm, respectively.

Azo compound **2b** is devoid of high-intensity chromophores in the region open for investigation. The (n,π*) transition is weak and highly structured, the strongest band (presumably the 0–0 transition) being located at 343 nm (ϵ 120 M^{-1} cm^{-1}). This fact required the use of relatively concentrated solution (0.1 M) and precluded the investigations of the absorption spectrum in pure hydrocarbon solvents due to precipitation upon cooling. Figure 2 displays the course of photolysis of **2b** (320 nm < λ < 390 nm, Corning 7-37) in EPA. Temperatures below 81 K were crucial to prevent thermal reaction of the primary photoproduct. An isosbestic point (323 nm) was observed during the first ca. 20% conversion only. Thus, secondary photolysis proved much more important for **2b** than in the case of **2a.** The two weak bands produced at 450 and 428 nm could be located in the very first spectrum recorded after short exposure. The absorption parameters associated with the primary photoproduct of **2b** can be seen in Table I. The extinction coefficients have been estimated in the same approximate manner as in the case of the diphenyl derivative. Slow warmup starting at 81 K and continuing to <95 K caused complete and irreversible disappearance of the spectrum of the photoproduct. The resulting spectrum showed a weak, broad band centered at 350 nm and a steep cutoff at 290 nm.

Information necessary for the assignment of the optical spectra was achieved by performing the photolysis of **2a** at 77 K in an ESR cuvette and placing it in a Dewar with liquid N_2 in the focal point of the Cary 17 spectrophotometer. Thus, it was possible to obtain ESR and UV/vis spectra (though distorted) from the *same* sample. The experiments proved that observation of the known ESR[6d] spectrum of **1a** was conditional upon the presence of the UV bands (Table I) and vice versa. The ESR spectrum and the UV/vis spectrum of **1a** are quite stable to prolonged irradiation of **1a** at 77 K. In contrast, the ESR spectrum and UV/vis spectrum of **1b** are unstable toward extended irradiation. These data provide further support for the identity of the UV and ESR carriers and suggest that **1a** enjoys relative stability toward irradiation (which is consistent with its high fluorescence yield, vide infra) whereas **1b** is rapidly consumed by secondary photolysis.

Emission Spectra. The fluorescence[5i,7] of the diazene **2a** is very weak and barely detectable ($\Phi_F \lesssim 10^{-3}$) in fluid as well as solid solution (77 K), while the diazene **2b** fluoresces with moderate efficiency ($\Phi_F \sim 0.01$). The emission spectrum of **2b** peaks at 352 nm, but the tail extends far into the visible.

After a brief period of photolysis, samples of **2a** and **2b** display an emission (Figure 3) that is due to photoexcitation of the photoproducts **1a** and **1b.** The lifetime of the emission (maxima at 485/510 nm) produced by photoexcitation of **1a** was determined to be 45 ± 5 ns. This lifetime when coupled with the relatively high quantum efficiency (~0.1–1.0) of this emission implies an inherent emission lifetime of 45–450 ns and, therefore, requires *that the luminescence from* **1a** *must be a fluorescence.* Such a lifetime implies an oscillator strength, *f*, of 10^{-2}–10^{-3}. The (fluorescent) emission of **1b** is much weaker (Φ_f(**1b**) ~ 10^{-4}–10^{-5}) than that of **1a.** Background and emission from impurities and secondary photolysis products proved a serious compli-

cation in the case of **1b** since it is far more photoactive than **1a** (Figures 1 and 2).

Excitation Spectra of 1a and 2a. Analyses of emission spectra at 77 K in glassy matrices are facilitated by the general applicability of the Kasha-Vavilov rule,[8] i.e., the emission quantum yield and the emission spectrum shape are independent of the wavelength used for excitation. For molecules whose absorbing and emitting states possess similar nuclear geometries a general rule is that the 0,0 bands of emission and absorption "overlap" in the sense that they correspond to a similar electronic energy gap. If, in addition to similar nuclear geometries, the absorbing and emitting states possess similar potential energy surfaces near the equilibrium shape, the absorption and emission spectra may display a mirror image relationship.[9] Since the most prominent vibrational progression present in an absorption or emission band generally is due to the vibration whose equilibrium position is most greatly changed by the radiative electronic transition, the prominent progression indicates the most important molecular distortion which occurs upon electronic transition.[10,11] A common vibration progression is suggestive and consistent with the possession of a common nuclear shape by the absorbing and emitting state.

A final and important rule allows correlation of an absorbing and emitting species. This rule[9] states that if the intensity of exciting light is kept constant as the frequency of the exciting light is varied, the emission intensity at any observed wavelength is proportional to ϵ, the molecular extinction coefficient of the absorbing species:

$$I_e = 2.3\epsilon c d I_0 \Phi_e \qquad (2)$$

where I_e is the observed emission intensity, I_0 is the total intensity of exciting light, ϵ = extinction coefficient of the absorbing species, c = concentration of the absorbing species, d = optical path length, and Φ_e = emission quantum yield. This rule (which is based on the Kasha-Vavilov[8] rule) is the basis of *emission excitation spectra.* To the extent that the rule is valid, a (true) excitation spectrum of photons emitted vs. exciting frequency corresponds to and *possesses the shape of the absorption spectrum of the species responsible for emission.* Luminescence techniques may thus be used to determine the "absorption spectra" of a molecule. Importantly, if the molecule under investigation possesses a high emission efficiency, its "absorption spectrum" may be measured at far lower concentrations than is possible with conventional absorption spectrometers. Excitation spectroscopy is also completely selective in that the "absorption spectrum" of a single luminescing component (present in a mixture of absorbing components) can be obtained.

The excitation spectra of the emissions from **1a** and **1b** are seen (Figure 3) to be in excellent (**1a**) to fair (**1b**) agreement with the absorption spectra (Figures 1 and 2). It has not been possible to locate the two weak visible absorptions in the excitation spectrum of **1b.** The emission described above disappeared irreversibly upon thawing and recooling of the glass.

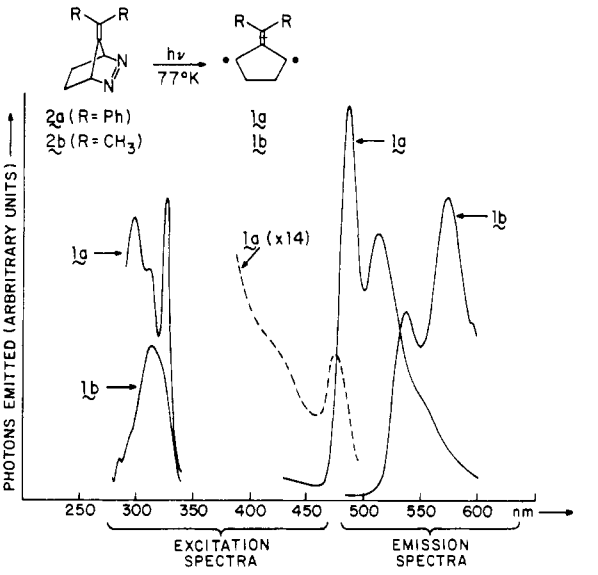

Figure 3. Emission and excitation spectra of irradiated solutions of **2a** and **2b** at 77 K in MCH. All intensities are arbitrary and do not reflect relative emission efficiencies. All spectra are corrected for instrumental response varying with wavelength. The dotted curve labeled **1a** (×14) is the excitation spectrum of **1a** in the longer wavelength region at 14 times the sensitivity of the excitation spectrum of **1a** at shorter wavelength.

Discussion

Figures 1 and 2 display the absorption spectra of photoproducts **1a** and **1b** at 77 K in glassy matrices. The observations of isosbestic points at 275 (**2a** → **1a**) and at 320 nm (**2b** → **1b**) during the initial stages of photolysis suggest that the short wavelength absorption is due to a single species. The observation of photochemically induced UV/vis and ESR spectra from the same sample is suggestive and consistent with the assignment of the triplet biradicals **1a** and **1b** (eq 1) as photoproducts.

The emission spectra produced upon photoexcitation of **1a** and **1b** occur very far "to the red" of the strong short-wavelength bands. Importantly, the very weak long-wavelength (350–450 nm) bands of **1a** possess overlapping 0,0 bands of absorption and emission. This overlap is shown clearly in Figure 3 for **1a,** i.e., the dotted line (excitation spectrum = absorption spectrum) and solid lines (emission) overlap in the region 460–480 nm. Comparison of Figure 1 and Figure 3 reveals the occurrence of similar vibrational progressions and a "mirror image" relationship of the long-wavelength absorption and emission bands of **1a.**[9] A similar situation of overlapping 0,0 bands for the long-wavelength absorption and emission is expected of **1b** but can only be qualitatively discerned. The competing absorption of **2b** and secondary product precludes definitive quantitative statements on this point.

One striking feature of the data in Table I is that the intensity, but not the position, of the bands in the 300–350-nm region seems to be influenced by replacing the methyl groups with phenyl. Usually, conjugation is accompanied by both deepening of the intensity and a bathochromic shift.[12] This rule of thumb, however, is obeyed for the long-wavelength absorptions. The increased Stokes shift observed when going from **1a** to **1b** either reflects a steeper potential energy surface governing the ground state of **1b** or a different equilibrium geometry of the excited state of **1b** relative to its ground state.[10,13] In either case, an average of the energies of the excitation and emission maxima provides a rough estimate of the energies of the relaxed excited states. This leads us to the value 59 kcal/mol for both compounds **1a** and **1b.**

Taken together, these data are completely consistent with the postulate that *the weak longer wavelength absorptions produced from photolysis of* **2a** *(and by analogy that of* **2b***) should be assigned to molecular structures possessing the same nuclear shapes as the related emitting species.* In other words, the shape of the species absorbing in the region 350–450 nm is deduced to be the same as the species emitting in the range 450–500 nm.

At this point, we consider two interpretations of our data. One interpretation states that the strong short-wavelength (250–350 nm) absorption bands, the weak long-wavelength (350–450 nm) absorption, and the emission bands all derive from a single common molecular structure or species. A second interpretation identifies the absorption at short wavelength with one species and the long-wavelength absorption and its associated emission with a second species.

Interpretation I. The Single Molecular Species Postulate. The most economical interpretation of our data is the postulate that in each case, a single molecular species of well-defined geometry is responsible for the observed ESR, absorption, and emission spectra that are generated by photolysis of **2a** and **2b** at 77 K. We consider first the possibility that this species is a triplet state of the TMM.

Experimental support for the assignment of a triplet ground state to the parent TMM[6e] as well as to **1a**[6d] and **1b**[6d] comes

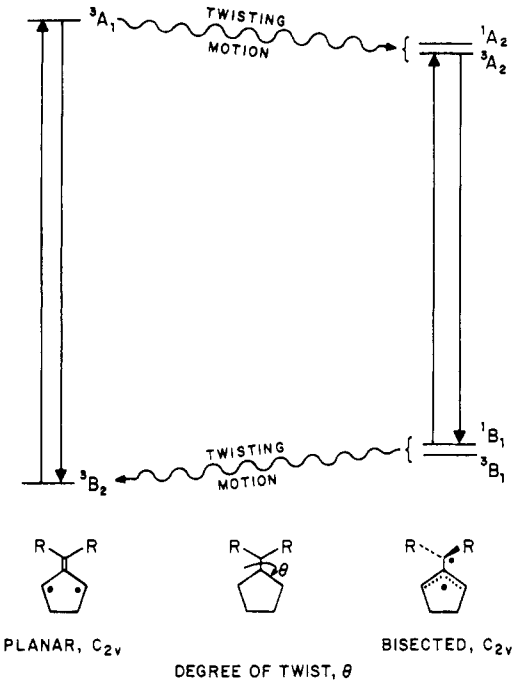

Figure 4. Schematic diagram of the interconversion of trimethylmethane species. Planar and bisected geometries are shown as specific possibilities.

from the observed Curie law dependence of the ESR signal intensity in each case. There is also convincing ESR spectroscopic evidence in the case of the parent TMM[6b] that all six protons are equivalent, a fact that can be simply (but not uniquely) explained by a planar configuration, in accord with theoretical prediction.[3g] Corresponding experimental evidence for planarity in **1a** and **1b** is not available, although a recent theoretical calculation[14] on a reasonably close model **1c** again predicts a planar triplet ground state. We assume here for the sake of argument that **1a** and **1b** triplets also are planar. Since we have shown that in both **1a** and **1b** the ESR and optical spectra have common carriers, the optical spectrum then would have to be interpreted as that of the planar triplet.

Considering the approximate value $f > 10^{-1}$ derived for the UV band of **1a** observed in the absorption spectra, the corresponding transition involved must be spin allowed, i.e., a planar upper triplet state is populated upon excitation. Davis and Goddard[3g] calculate the energy of the lowest excited triplet state of parent TMM to be 108 kcal/mol above the ground state (corresponding to a transition at 266 nm) and find this value to be independent of whether the species is assumed to have D_{3h} ($^3E'$) or C_{2v} ($^3B_2$ and $^3A_1$, degenerate) symmetry.

The predicted value[3g] of 108 kcal/mol for the planar triplet is not in good agreement with excitation energies implied by the long-wavelength bands observed for **1a** and **1b** (~60 kcal/mol). It is conceivable that the incorporation of a trimethylenemethane unit into a five-membered ring could cause narrowing of the spacing of the two lowest triplets as compared to that in the parent compound. However, the energy change would have to be unexpectedly large (~49 kcal/mol) to account for the discrepancy.

There is also some difficulty in fitting the absorption and emission intensities to the model of a planar triplet as the sole source of the spectrum. Theory[3g] predicts an oscillator strength of $f \gtrsim 10^{-3}$ ($\epsilon_{max} \gtrsim 10^2$) for the lowest energy $^3B_2$ (planar) $\rightarrow$ $^3A_1$ (planar) transition of parent TMM. Interpretation I identifies the visible absorption of **1a** and **1b** with this transition. The weakness of the visible absorption of **1a** and **1b** allows establishment of a limit of $f < 10^{-4}$ if a single species is postulated to be the exclusive carrier of the absorption strength. On the other hand, the measurements of the fluorescence lifetime and quantum yield for **1a** lead to the value of $f \gtrsim 10^{-1}$–10^{-3} for the oscillator strength of the emitting state. (It must be emphasized that the experimental difficulties already described prevent us from applying this argument in the case of **1b**).

As we have noted, the overlap of the 0,0 absorption and emission bands requires that the ground and excited states have very similar geometry. Under these conditions, the Strickler–Berg relationship[15] may be applied, and we may conclude that the f numbers for absorption and emission should be the same. The quantitative disagreement between the derived f numbers for absorption and emission thus is inconsistent with a single species.

The single species interpretation cannot readily be rescued by attributing the spectrum to a planar singlet ($^1A_1$ or $^1B_1$), since these are both predicted[3g] to have λ_{max} 289 nm for the lowest lying optical transition in the case of the parent TMM. The prediction of λ_{max} 359 nm for a *bisected* triplet species, in which one of the methylene groups has been twisted by 90° with respect to the plane of the other two, is in better agreement with the observed long-wavelength absorption. Note that the calculations[3g] suggest that the planar parent TMM triplet should be 18–20 kcal/mol more stable than the bisected triplet, which would preclude any appreciable absorption by the latter. Thus, the assignment of a significant role to the bisected triplet, either as the sole carrier of the spectrum (interpretation I) or as one of two absorbing species (interpretation II, see below), requires either a large substituent effect on the planar-bisected energy spacing or some other theoretical adjustment.

For most of the variants of interpretation I to be correct, the theoretical calculation of transition energy must be in serious error or the substituent effects must be unexpectedly large. For the case of the bisected triplet, the transition energy is in reasonable agreement with that calculated. However, all of the variants of interpretation I suffer from the inconsistency of the f value for the visible absorption with that derived from the emission.

We feel that economy of interpretation is insufficient reason to justify adherence to interpretation I. We therefore seek a more satisfactory alternative.

Interpretation II. The Two Molecular Species Postulate. The triplet species that carries the ESR spectrum is responsible for the strong UV absorption of the diphenyl diyl **1a,** a $^3B_2$ (C_{2v}, planar) $\rightarrow$ $^3A_1$ (C_{2v}, planar) electronic transition with a 0,0 band near 330 nm, but the weak visible absorption and emission are caused by the presence of a second electronic and/or geometric structural form of **1a** in thermal equilibrium with the triplet. The nature of this second species cannot be specified from the spectroscopic data themselves, but it seems clear that it must have the same *constitution* as the triplet since its optical spectra can be observed when and only when the characteristic ESR signal is observed. A similar interpretation could be applied to the data on the dimethyl system, **1b.**

Among the several candidate structures for the second species, especially in the case of **1b,** is the trappable singlet that results from the thermal or direct photochemical deazetation of **2b**.[5d-g] It has been shown[5j,6d] that the upper limit of the energy spacing between this species and the ground-state triplet lies between 0.6 and 3.5 kcal/mol. Thus, unless the extinction coefficient were especially small, it would not be unreasonable to expect this singlet to contribute to the optical spectrum, even at 77 K.

Although it has been speculated[5d] that the trappable dimethyl singlet diyl **1b** has a bisected configuration, with the CMe_2 group perpendicular to the ring, later work[5k,l] on the corresponding dihydrogen diyl **1c** has favored a planar species as the reactive form. In any case, theory suggests[3] that, at least for the parent TMM itself, the energy difference between the

planar and bisected singlets probably is small. It is conceivable, therefore, that the optical absorption spectra could receive contributions from both a planar and a bisected form. Perhaps even the hydrocarbon systems derived hypothetically from ring closure (bicyclo[3.1.0]hex-1-ene or 5-methylenebicyclo-[2.1.0]pentane) may contribute.

The 0,0 transitions observed near 330 nm for the planar triplets **1a** and **1b** presumably are displaced to longer wavelengths than that predicted[3g] (266 nm) for parent TMM by substituent effects. On this basis, one might expect a similar shift in the spectrum of the "second species". This would be consistent with the observed position of the long-wavelength bands (450–500 nm) as compared to the predicted[3g] absorption at 359 nm for the bisected TMM species, singlet or triplet. We therefore tentatively assign the long-wavelength visible absorption to a vertical transition ($^3B_1 \rightarrow {}^3A_2$ or $^1B_1 \rightarrow {}^1A_2$) and the emission to a fluorescence process ($^3A_2 \rightarrow {}^3B_1$ or $^1A_2 \rightarrow {}^1B_1$) in the bisected species. The concentration of this species is unknown, so that the f value of the absorption cannot be determined and compared to theory.

The observation (Figure 3) that the excitation spectrum for emission includes not only the long-wavelength visible absorption bands but also the strong UV bands of both **1a** and **1b** is especially noteworthy. If our tentative assignments of the UV absorption to the planar triplet and the visible to a bisected species are correct, it follows that in the excited state, torsion about the exocyclic partial double bond of diyls **1a** and **1b** can result in large conformational changes. This behavior can be described schematically as shown in Figure 4.

The scheme shown in Figure 4 would suggest that the theoretical calculations,[3g] modified for reasonable substituent effects, account rather well for the optical transitions. For the present, it is not clear how to reconcile the discrepancy of about 18–20 kcal/mol between the predicted *ground state* planar-bisected gap and the much smaller one needed for consistency with the two-species interpretation. Further theoretical studies may be useful in this regard.

If any planar singlet species is present, theory suggests that its allowed transition should occur at shorter wavelength than that of the bisected species.[3g] Since the planar triplet also absorbs strongly in the shorter wavelength region, direct spectroscopic detection of the planar singlet may not be easy.

The absorption and emission properties of **1a** and **1b** are qualitatively similar. Perhaps the most noteworthy difference is the larger Stokes shift in the case of the visible absorption of **1b.** Any interpretation must be speculative at this time, but a rationalization could be based upon the idea that the change in equilibrium geometries of the so-called "bisected" species upon excitation may be different in **1b** and **1a.** This would be true in general, for example, if the angle of twist of the exocyclic group is not required to be strictly 90° in both instances.

In principle, if $\Delta H \neq 0$, it should be possible to confirm the postulate of two absorbing species in thermal equilibrium by observing a temperature dependence of the spectrum.

Conclusion

Our data are completely consistent with the conclusion that biradicals of constitution formulas **1a** and **1b** are formed in the photolysis of **2a** and **2b,** respectively, at temperatures near 77 K. Theoretical calculations on TMM are in poor agreement with the postulate that a single molecular structure is the carrier of the ESR, UV/vis, and emission spectra observed when **2a** and **2b** are photolyzed. The single molecular species postulate also results in a substantial disagreement between the experimental oscillator strengths derived from independent absorption and emission measurements. The postulate that a planar triplet species is the carrier of the ESR spectrum and the strong UV absorption and that a (low concentration of a) second species is responsible for the weak visible absorption and the emission is consistent with all of our experimental data and is in better agreement with theoretical calculations than the single species postulate. The energy difference between the two species must be small, since both are contributing to the optical spectra, even at 77 K.[16,17]

Acknowledgments. The authors at Columbia University thank the Air Force Office of Scientific Research (Grants AFOSR-74-2589E and AFOSR-78-3502) and the National Science Foundation (Grants NSF-CHE-73-04672 and NSF-CHE-76-15890) for their generous support of this research. Niels Harrit acknowledges a travel grant from the Danish National Science Foundation and Manfred Mirbach acknowledges a NATO Postdoctoral Fellowship for 1976–1977. The authors at Yale University thank the National Science Foundation (Grant CHE-76-00416), the National Institute of General Medical Sciences (Grant GM-23375), and the Camille and Henry Dreyfus Foundation. The assistance of D. R. Kelsey and K. Rabin is gratefully acknowledged. The authors are greatly indebted to Dr. Angelo Lamola of Bell Laboratories for generous access to the apparatus required for quantitative absorption measurements near 77 K, and to Mr. Frank Dolieden of Bell Laboratories for his technical advice and assistance. We also thank Dr. W. W. Schoeller for an advance copy of his paper (ref 14) and Professor Josef Michl for helpful comments.

References and Notes

(1) (a) Columbia University; (b) Yale University.
(2) P. Dowd, *Acc. Chem. Res.*, **5,** 242 (1972).
(3) (a) E. R. Davidson and W. T. Borden, *J. Am. Chem. Soc.*, **99,** 2053 (1977); (b) *J. Chem. Phys.*, **64,** 663 (1976); (c) W. T. Borden, *J. Am. Chem. Soc.*, **98,** 2695 (1976); (d) B. K. Carpenter, R. D. Little, and J. A. Berson, *ibid.*, **98,** 5723 (1976); (e) W. J. Hehre, L. Salem, and M. R. Willcott, *ibid.*, **96,** 4328 (1974); (f) D. R. Yarkony and H. F. Schaefer, *ibid.*, **96,** 3754 (1974); (g) J. A. Davis and W. A. Goddard, III, *ibid.*, **99,** 4242 (1977); (h) W. T. Borden and E. R. Davidson, **99,** 4587 (1977).
(4) J. D. Roberts, "Notes on Molecular Orbital Calculation", W. A. Benjamin, New York, N.Y., 1961, p 56; (b) A. Streitwieser, "Molecular Orbital Theory for Organic Chemists", Wiley, New York, N.Y., 1961, pp 43, 57; (c) W. T. Borden, "Modern Molecular Orbital Theory for Organic Chemists", Prentice-Hall, Englewood Cliffs, N.J., 1975.
(5) (a) M. Schneider, *Angew. Chem., Int. Ed. Engl.*, **14,** 707 (1975); (b) R. J. Crawford, D. M. Cameron, and H. Tokunaga, *Can. J. Chem.*, **52,** 4025 (1974); (c) R. J. Crawford and H. Tokunaga, *ibid.*, **52,** 4033 (1974); (d) J. A. Berson, L. R. Corwin, and J. H. Davis, *J. Am. Chem. Soc.*, **96,** 6177 (1974); (e) J. A. Berson, C. D. Duncan, G. C. O'Connell, and M. S. Platz, *ibid.*, **98,** 2358 (1976); (f) J. A. Berson, C. D. Duncan, and L. R. Corwin, *ibid.*, **96,** 6175 (1974); (g) J. A. Berson, D. M. McDaniel, and L. R. Corwin, *ibid.*, **94,** 5509 (1972); (h) M. S. Platz and J. A. Berson, *ibid.*, **98,** 6743 (1976); (i) M. S. Platz, D. R. Kelsey, J. A. Berson, N. J. Turro, and M. J. Mirbach, *ibid.*, **99,** 2009 (1977); (j) M. S. Platz and J. A. Berson, *ibid.*, **99,** 5178 (1977); (k) R. Siemionko, A. Shaw, G. O. Connell, R. D. Little, B. K. Carpenter, L. Shen, and J. A. Berson, *Tetrahedron Lett.*, 3529 (1978); (l) J. A. Berson, *Acc. Chem. Res.*, in press.
(6) (a) P. Dowd, *J. Am. Chem. Soc.*, **88,** 2587 (1966); (b) P. Dowd and K. Sachdev, *ibid.*, **89,** 715 (1967); (c) J. A. Berson, R. J. Bushby, J. M. McBride, and M. Tremelling, *ibid.*, **93,** 1544 (1971); (d) M. S. Platz, J. M. McBride, R. D. Little, J. J. Harrison, A. Shaw, S. E. Potter and J. A. Berson, *ibid.*, **98,** 5725 (1976); (e) R. J. Baseman, D. W. Pratt, M. Chow and P. Dowd, *ibid.*, **98,** 5726 (1976); (f) H. Yoshida and O. Edlund, *Chem. Phys. Lett.*, **42,** 107 (1976); (g) P. Dowd and M. Chow, *J. Am. Chem. Soc.*, **99,** 2825 (1977); (h) P. Dowd and M. Chow, *ibid.*, **99,** 6438 (1977).
(7) For a discussion of the absorption and emission spectroscopy of cyclic azoalkanes see M. J. Mirbach, M. F. Mirbach, K. C. Liu, W. R. Cherry, N. J. Turro, and P. S. Engel, *J. Am. Chem. Soc.*, **100,** 5122 (1978).
(8) J. B. Birks, "Photophysics of Aromatic Molecules", Wiley, New York, N.Y., 1970, p 142; M. Kasha, *Discuss. Faraday Soc.*, **9,** 14 (1950).
(9) C. A. Parker, *Adv. Photochem.*, **2,** 305 (1964).
(10) N. J. Turro, "Modern Molecular Photochemistry", W. A. Benjamin/Cummings, Menlo Park, Cal., 1978.
(11) H. Suzuki, "Electronic Absorption Spectra and Geometry of Organic Molecules", Academic Press, New York, N.Y., 1967, p 79 ff.
(12) E. S. Stern and C. J. Timmons, "Electronic Absorption Spectroscopy", Arnold, London, 1970, p 31.
(13) P. Pringsheim, "Fluorescence and Phosphorescence", Interscience, New York, N.Y., 1963, p 556.
(14) W. W. Schoeller, *J. Chem. Soc., Perkin Trans. 2,* in press.

(15) F. J. Strickler and R. A. Berg, *J. Chem. Phys.*, **37**, 814 (1962).
(16) For a recent report of the optical spectra of a biradical interpreted with two species, see J.-F. Muller, D. Muller, H. J. Dewey, and J. Michl, *J. Am. Chem. Soc.*, **100**, 1629 (1978).
(17) In principle, a determination of the equilibrium constant would be possible if the extinction coefficients for each species were available. Unfortunately, they are not, and it should be borne in mind that the ϵ values cited in Table I depend upon the assumptions already stated.

Pyridinyl Radicals, Pyridinyl Anions, Z Values, and Disproportionation Equilibria

Mahboob Mohammad,* A. Y. Khan, M. Iqbal, R. Iqbal, and M. Razzaq

Contribution from the Electrochemistry Group, Department of Chemistry, Quaid-i-Azam University (University of Islamabad), Islamabad, Pakistan. *Received April 12, 1978*

Abstract: In order to understand the mechanism of a reaction of biological importance, electrochemical investigations were carried out on 1-ethyl-4-carbomethoxypyridinium iodide and 1,1-trimethylenebis(4-carbomethoxypyridinium) iodide (1:3:1) in a number of solvents. First and second reductions were recorded using triangular wave cyclic voltammetry in a three-electrode configuration, yielding information regarding the stabilities of the various reduction products. Through these investigations, it is established that the 1-ethyl-4-carbomethoxypyridine anion exists as a stable species, which may be responsible for some fast reactions of pyridinyl radicals. It was also found that the cation radical and diradical formed with relative ease by electrochemical reduction of 1:3:1 salt. These radicals are stable on the electrochemical time scale. However, the higher reduction process is slow. This enabled the calculation of the heterogeneous rate constant. The disproportionation equillibria (a) $2py\cdot \rightleftarrows py^+ + py^-$ and (b) $2\,(1:3:1)^{+}\cdot \rightleftarrows (1:3:1)^{2+} + (1:3:1)$: were studied and equilibrium constants were calculated from the cyclic voltammogram. The relationship between the disproportionation equilibrium constant and Z values was investigated.

The study of pyridinyl radicals resulted in advancing our understanding toward reactions of biological importance. Kosower, in a recent review article,[1] has described some of the pyridinyl radicals, diradicals, and other related cation radicals. He has also discussed studies on their chemical and physical properties and their importance in biological reactions. One such study, presumably, leads to the understanding of the herbicidal property of methylviologen (paraquat) dichloride, etc. During the investigation of the properties of pyridinyl radicals, 1-ethyl-4-carbomethoxypyridinyl, it was found that some of the properties, e.g., higher reduction and disproportionation, may have relevance in biological or other reactions.

A widely and commonly studied pyridinyl radical is 1-ethyl-4-carbomethoxypyridinyl (I, py·),[1] owing to the ease with which it can be generated and studied: the radical is stable in acetonitrile in the absence of oxygen. Less familiar radicals

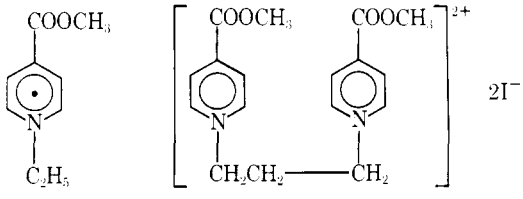

I II

are those derived from 1,1-trimethylenebis(4-carbomethoxypyridinium) diiodide (II).[1,3] Because of difficulty in the preparation and relative instability, radicals derived from II have been less studied. However, spectroscopic studies on the cation radical and diradical from II and their metal complexing properties have been made.[3,4]

Historically, the stability of pyridinyl radical I was first discovered in the electrochemical reduction of the pyridinium salt.[5] However, further electrochemical studies have not been carried out to any great extent. Mackay et al.[6] have studied the relationship of one-electron reduction potentials and the longest wavelength charge transfer band of 1-alkylpyridinium iodide. Measurements were, however, carried out with a two-electrode system and no attempt was made to study the second reduction potential of such systems. Other electrochemical studies are based upon generating the pyridinyl radical on a hanging mercury drop electrode, reacting it with various substrates, and calculating the rate constant for the bimolecular reaction by the method developed by us.[7,8]

The existence of py^- had been proposed by Kosower[9] as a py^+, py^- ion pair. The existence of free py^- has never been reported and the disproportionation equilibria

$$2py\cdot \overset{K}{\rightleftarrows} py^+ + py^- \qquad (1)$$

have never been studied, although the mediating properties of this species in a reaction like protonation of pyridinyl radical[8] are very plausible.[10]

It has been mentioned above that some of the properties of cation radicals and diradicals from II have been reported[3,4] but no electrochemical investigation has been carried out so far. Thus, it seems worthwhile to investigate the stability of mono- and diradicals produced by electrochemical reduction in various solvents and to investigate the possibility of existence of higher reduction products.

In this report, the results of our electrochemical investigation[3] of the salts of I and II in various solvents, encompassing the reduction potential, the stability of reduction products, disproportionation equilibria, and Z values, are presented.

Results and Discussion

Electrochemical measurements (triangular wave cyclic voltammetry) were carried out at a hanging mercury drop electrode, with (in most cases) tetra-*n*-butylammonium perchlorate as supporting electrolyte. These results are collected in Tables I–III.

It is clear from Table I that the reduction potential for the process given in eq 2 increases as the Z values increase.

$$py^+I^- + e \rightleftarrows py\cdot + I^- \qquad (2)$$

This seems obvious, since higher Z values of a solvent mean its greater stabilizing property for the ion pair; hence it would be more difficult to reduce the ion or ion pair. However, this point should not be overemphasized since correction for liquid

0002-7863/78/1500-7658$01.00/0